

# High-Performance Carbon Fibers Prepared by Continuous Stabilization and Carbonization of Electron Beam-Irradiated Textile Grade Polyacrylonitrile Fibers

Simon König, Volker Bauch, Christian Herbert, Andreas Wego, Mark Steinmann, Erik Frank, and Michael R. Buchmeiser\*

The manufacturing of high-performance carbon fibers (CFs) from low-cost textile grade poly(acrylonitrile) (PAN) homo- and copolymers using continuous electron beam (EB) irradiation, stabilization, and carbonization on a kilogram scale is reported. The resulting CFs have tensile strengths of up to  $3.1 \pm 0.6$  GPa and Young's moduli of up to  $212 \pm 9$  GPa, exceeding standard grade CFs such as Toray T300. Additionally, the Weibull strength and modulus, the microstructure, and the morphology of these CFs are determined.

## 1. Introduction

Over the last 50 years, the applications for carbon fibers (CFs) expanded from aerospace and military to wind energy, sporting goods, automotive, and construction. Concomitantly, the production costs for standard CFs have fallen by approximately two orders of magnitude.<sup>[1–11]</sup> The CF market is expected to have an annual growth of at least 10 % over the next few years, with a huge additional potential for demand in the automotive and construction industry in case the price can be further substantially, i.e., to  $<10$  \$ kg<sup>-1</sup>.<sup>[5]</sup>

More than 90% of the global CF production is derived from the precursor poly(acrylonitrile) (PAN), the remainder being pitch. CFs based on alternative precursors like lignin, cellulose, or

polyolefins have not yet been commercialized since they still do not meet the mechanical properties of PAN- or pitch-based CFs; nonetheless, they are extensively researched.<sup>[12–18]</sup>

For PAN-based CF production, special “CF-PAN” fibers with high number-average molecular weights,  $M_n > 120\,000$  g mol<sup>-1</sup> and low comonomer content of 1–3 mol% are used.<sup>[3,19–21]</sup> Comonomers, e.g., methyl acrylate or methyl methacrylate, are employed to facilitate spinning,


other comonomers such as itaconic acid or methacrylic acid are employed to lower the onset temperature  $T_{\text{onset-S}}$  of cyclization and dehydrogenation reactions commonly referred to as stabilization. Costs for PAN-based precursor fibers are typically  $>7$  \$ kg<sup>-1</sup>, they make up approximately 50 % of the total CF production costs.<sup>[8,10,22]</sup>

PAN fibers for CFs represent only 10–20% of the total PAN fiber production, the other 80–90 % of PAN are used for textile applications, e.g., for clothing, carpets, or awnings.<sup>[23]</sup> These textile grade “Tex-PAN” fibers usually have a lower  $M_n$  of around 40 000–100 000 g mol<sup>-1</sup> and a comonomer content of 3–7 mol% in order to increase productivity by increasing polymer concentration in the spinning dope.<sup>[23]</sup> Typical comonomers include methyl acrylate, vinyl acetate, or methyl methacrylate, as well as comonomers that facilitate fiber dyeing like sodium methallyl sulfonate. Due to their high spinning productivity and energy efficiency, costs for Tex-PANs are typically between 2–4 \$ kg<sup>-1</sup>.<sup>[24]</sup> Consequently, the total costs for CF production could be reduced by ca. 20–25% if Tex-PAN fibers instead of CF-PAN fibers could be used as precursors.

However, the use of Tex-PANs as CF precursor entails challenges, such as their thermal properties. Tex-PANs have only a small temperature window for stabilization,  $\Delta T_s$ , of  $\approx 15$ –50 °C between  $T_{\text{onset-S}}$  and the temperature of the maximum exotherm of the stabilization reaction,  $T_{\text{max-S}}$ , whereas  $\Delta T_s$  is between 50 and 100 °C for CF-PAN. Consequently, Tex-PAN has a high risk of burning during stabilization due to this narrow processing temperature window, especially in the center of large tows, where the heat transfer is low. This challenge can be overcome by alternative stabilization techniques like plasma- or microwave-assisted stabilization,<sup>[24–26]</sup> or by altering the thermal properties of the precursor by chemical modification, ultraviolet irradiation, gamma irradiation, or electron beam (EB) irradiation, so that  $T_{\text{onset-S}}$  is shifted to lower temperatures.<sup>[25,27–36]</sup> The irradiation methods

S. König, M. R. Buchmeiser  
 Institute of Polymer Chemistry  
 University of Stuttgart  
 Pfaffenwaldring 55, Stuttgart D-70569, Germany  
 E-mail: michael.buchmeiser@ipoc.uni-stuttgart.de

S. König, V. Bauch, M. Steinmann, E. Frank, M. R. Buchmeiser  
 German Institutes of Textile and Fiber Research  
 Körschtalstr. 26, Denkendorf D-73770, Germany  
 C. Herbert, A. Wego  
 Dralon GmbH  
 Chempark Dormagen  
 Postfach 10 04 85, Dormagen 41522, Germany

 The ORCID identification number(s) for the author(s) of this article can be found under <https://doi.org/10.1002/mame.202100484>

© 2021 The Authors. Macromolecular Materials and Engineering published by Wiley-VCH GmbH. This is an open access article under the terms of the Creative Commons Attribution License, which permits use, distribution and reproduction in any medium, provided the original work is properly cited.

DOI: 10.1002/mame.202100484

**Table 1.** Mechanical properties of the utilized Tex-PAN fibers.

Fiber type	Tensile strength [cN per tex]	Tensile strength [MPa]	Young's modulus [cN per tex]	Young's modulus [MPa]	Elongation [%]	Diameter [ $\mu\text{m}$ ]
Tex-PAN 1 dry-spun	36 $\pm$ 4	420 $\pm$ 50	820 $\pm$ 40	9.7 $\pm$ 0.5	16.8 $\pm$ 2.7	12.1 $\pm$ 0.8
Tex-PAN 1 wet-spun	46 $\pm$ 3	540 $\pm$ 30	960 $\pm$ 80	11.4 $\pm$ 0.9	12.3 $\pm$ 0.8	12.1 $\pm$ 3.0
Tex-PAN 2	46 $\pm$ 4	550 $\pm$ 50	1020 $\pm$ 50	12.0 $\pm$ 0.6	12.1 $\pm$ 1.3	12.1 $\pm$ 0.5
Tex-PAN 3	52 $\pm$ 3	610 $\pm$ 40	1000 $\pm$ 50	11.9 $\pm$ 0.6	12.1 $\pm$ 1.0	13.6 $\pm$ 1.0

lower  $T_{\text{onset-S}}$  by forming persistent radicals in PAN, mainly in the backbone. These radicals can initiate stabilization reactions upon heating.  $T_{\text{max-S}}$  is not affected that much, consequently, the processing temperature window can be sufficiently widened.<sup>[27,37,38]</sup> EB-irradiation is especially useful, as the necessary irradiation time is the shortest, ranging from seconds to minutes, depending on the employed EB irradiation dose and the irradiation rate.<sup>[35]</sup>

Yoo et al. recently reported on discontinuous EB irradiation, stabilization, and carbonization of a Tex-PAN with 10.7 wt% (6.9 mol%) vinyl acetate as comonomer.<sup>[36]</sup> The resulting CFs had a tensile strength of 1.8 GPa and a Young's modulus of 147 GPa. Unfortunately, with these fibers the cost advantage of using Tex-PAN as a precursor is outweighed by the low strength and modulus of the resulting CFs, since standard grade CFs typically have at least a tensile strength of 3 GPa and a Young's modulus >200 GPa.

The low mechanical properties probably stem from the high comonomer content, since Yoo et al. observed filament fusion when carbonizing unirradiated textile PAN, which Sedghi et al. did not observe when carbonizing untreated Tex-PANs with lower comonomer content.<sup>[39]</sup> Furthermore, the question of whether EB-irradiation of PAN "only" allows for a reduced stabilization temperature/stabilization time, or whether CFs made from EB-irradiated PAN also have better mechanical properties than CFs made from the corresponding unirradiated PAN is of high interest. Recently, such comparisons concluded that the EB-irradiation leads to CFs with poor mechanical properties.<sup>[32,40]</sup>

Here, the continuous EB-irradiation, stabilization and carbonization of Tex-PANs on a kilogram scale is reported. The resulting CFs had up to 3.1 GPa tensile strength and 212 GPa Young's modulus, rendering them a viable low-cost alternative to standard CFs like the Toray T300 fiber, which reportedly has a tensile strength of 3.5 GPa and Young's modulus of 230 GPa (tensile strength = 3.0 GPa and Young's modulus = 197 GPa measured on our equipment). The CFs derived from irradiated Tex-PANs were compared to the corresponding CFs derived from unirradiated Tex-PANs, while keeping processing parameters like the stabilization time, carbonization time, and stretching constant.

## 2. Results and Discussion

The low-cost textile-grade PAN-copolymers Tex-PAN 1, Tex-PAN 2, and the homopolymer Tex-PAN 3 are widely used for textiles like clothing or carpets. Tex-PAN 3 is a homopolymer, therefore spinning of Tex-PAN 3 fibers is more challenging due to its lower solubility. Nevertheless, Tex-PAN 3 could be an interesting precursor polymer for CFs, too, since it is well known that the mechanical properties of the final CFs improve with decreasing comonomer content in the PAN precursor fiber.<sup>[21,41]</sup> No-

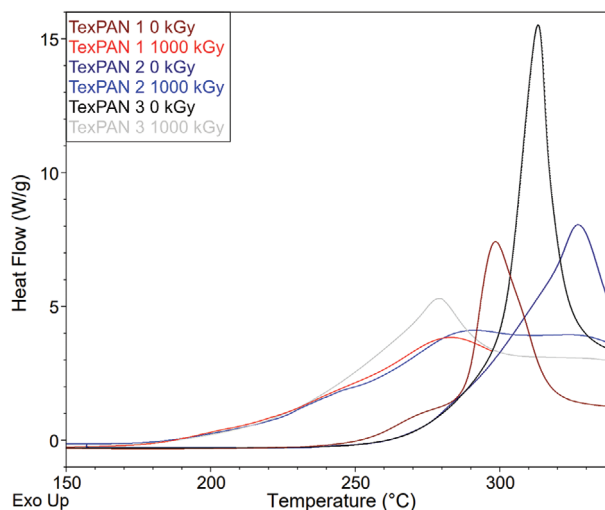


**Figure 1.** DSC measurements in air of the Tex-PAN fibers, before and after irradiation.

tably, this rule currently only applies to a minimum of approximately 1 mol% of a stabilization-inducing comonomer, e.g., itaconic acid.<sup>[42]</sup> Untreated PAN-homopolymers are not suitable for CF production, as they show a very strong exotherm at  $T_{\text{max-S}}$ , a high  $T_{\text{onset-S}} \approx 300$  °C and a small temperature gap  $\Delta T_S$  between  $T_{\text{onset-S}}$  and  $T_{\text{max-S}}$  of 15–20 °C. However, the  $T_{\text{onset-S}}$  of PAN can be lowered by EB-irradiation, thus, a Tex-PAN 3-fiber with thermal properties comparable to those of typical CF-PANs can be obtained. **Table 1** shows the mechanical properties of the Tex-PAN fibers used.

Tex-PAN 1 fibers were both dry- and wet-spun, Tex-PAN 2 and Tex-PAN 3 were wet-spun. Young's modulus, tensile strength, and elongation of the wet-spun fibers were at the lower end of the typical range for CF precursors. The dry-spun Tex-PAN 1 fibers were slightly less stretched and therefore had a higher residual elongation and lower tensile strength and Young's modulus.

### 2.1. Thermal Properties of Unirradiated and EB-Irradiated Tex-PAN 1, Tex-PAN 2, and Tex-PAN 3 Fibers

**Figure 1** shows DSC measurements of Tex-PAN 1, Tex-PAN 2, and Tex-PAN 3 fibers at an EB dose of 0 and 1000 kGy, respectively, the corresponding values for  $T_g$ ,  $T_{\text{onset-S}}$ ,  $T_{\text{max-S}}$ , and  $\Delta T_S$  are summarized in **Table 2**.

EB-irradiation substantially equalizes the thermal properties ( $T_g$ ,  $T_{\text{onset-S}}$ ,  $T_{\text{max-S}}$ ) of the three Tex-PANs, which differed significantly before irradiation, resulting in very similar values

**Table 2.** Overview of the thermal properties ( $T_g$ ,  $T_{\text{onset-S}}$ , and  $T_{\text{max-S}}$ ) of unirradiated and irradiated wet-spun Tex-PAN fibers.

PAN	EB-Dose [kGy]	$T_g$ [°C]	$T_{\text{onset-S}}$ [°C]	$T_{\text{max-S}}$ [°C]	$\Delta T_S$ [°C]
Tex-PAN 1	0	104	250	298	48
Tex-PAN 1	1000	n. d. <sup>a)</sup>	204	286	82
Tex-PAN 2	0	108	256	314	58
Tex-PAN 2	1000	n. d. <sup>a)</sup>	206	289	83
Tex-PAN 3	0	104	298	313	15
Tex-PAN 3	1000	n. d. <sup>a)</sup>	216	280	64

<sup>a)</sup> not determinable, no  $T_g$  was observed.

after applying an EB dose of 1000 kGy. After EB treatment,  $\Delta T_S$  increased significantly for all Tex-PANs, most significantly for Tex-PAN 3. There, EB irradiation resulted in an increase in  $\Delta T_S$  by of more than 400% compared to unirradiated PAN.

From the irradiated PANs, no  $T_g$  could be determined; instead, a weakly exothermic signal was visible between 80 and 120 °C (Figure S4, Supporting Information). This can be attributed to radical recombination reactions in the amorphous regions occurring above  $T_g$ . At an EB-dose of 1000 kGy,  $T_{\text{onset-S}}$  was 204 °C for Tex-PAN 1, 206 °C for Tex-PAN 2, and 216 °C for Tex-PAN 3.  $T_{\text{onset-S}}$  was thus in the range of commercial PAN precursor fibers at this EB dose ( $T_{\text{onset-S CF-PAN}} \approx 200\text{--}240$  °C). Figure S16 (Supporting Information) shows a comparison between the irradiated Tex-PAN with a commercial PAN precursor fiber.

## 2.2. Oxidative Thermal Stabilization

Stabilization was carried out in a stabilization oven with four heating zones (Figure S1, Supporting Information). The temperatures in the heating zones were adjusted to the thermal properties of the PAN-fiber used. In all stabilization trials with both irradiated and unirradiated PAN, a temperature similar to  $T_{\text{onset-S}} \pm 10$  °C was used in the first heating zone. Generally, if the temperature is chosen too high, inhomogeneous stabilization or core-sheath formation may occur.<sup>[43]</sup> In the worst case, overheating leads to the incineration of the fibers inside the stabilization furnace due to the exothermic, autocatalytic nature of the PAN cyclization reaction.

A temperature between 265 and 280 °C was selected as the final temperature for stabilization (heating zone 4), which usually leads to densities of the resulting OxPAN fibers between 1.35 and 1.39 g mL<sup>-1</sup> and thus to CFs with good mechanical properties.<sup>[44]</sup> The stabilization temperature was chosen such that the density of the OxPAN fibers was in the range of 1.35–1.39 g mL<sup>-1</sup>.

**Table 3** summarizes the temperature profiles and stretch ratios during the stabilization trials with both unirradiated and irradiated Tex-PAN. For a given Tex-PAN, stretching was kept constant in all the stabilization trials. For Tex-PAN 1, a stretching of 5% both in heating zones 1 and 2 was applied.

Furthermore, Table 3 shows the tensile forces that occurred in the different heating zones. The irradiated Tex-PAN 1 and Tex-PAN 2 fibers built up significantly higher tensile forces in each heating zone than the unirradiated Tex-PAN 1 and Tex-PAN 2 fibers. Comparable tensile forces could not be achieved with

**Table 3.** Temperature profile, tensile force, and stretching in the four heating zones of the stabilization furnace during stabilization of the unirradiated and irradiated Tex-PAN fibers.

	Heating zone				
		1	2	3	4
Tex-PAN 1	Stretching [%]	5	5	0	0
		0 kGy			
	Temperature [°C]	240	250	265	275
		Tensile force [cN]			
	Temperature [°C]	210	225	245	265
		Tensile force [cN]			
1000 kGy (dry-spun)	Temperature [°C]	210	225	245	265
	Tensile force [cN]	196	268	272	274
Tex-PAN 2	Stretching [%]	5	0	0	0
		0 kGy			
	Temperature [°C]	250	260	270	280
		Tensile force [cN]			
	Temperature [°C]	210	225	245	270
		Tensile force [cN]			
1000 kGy	Temperature [°C]	293	230	254	245
	Tensile force [cN]	293	230	254	245
Tex-PAN 3	Stretching [%]	2	0	-0.5	-0.5
		0 kGy			
	Temperature [°C]	255	265	270	275
		Tensile force [cN]			
	Temperature [°C]	210	225	245	265
		Tensile force [cN]			
1000 kGy	Temperature [°C]	210	225	245	265
	Tensile force [cN]	583	539	517	522

unirradiated Tex-PAN 1 and Tex-PAN 2 fibers. For unirradiated Tex-PAN 1 fibers, the multifilament ruptured completely at  $\approx 240$  cN and 30% stretching in the first heating zone. The higher tensile forces during the stabilization of the irradiated fibers are attributed to intermolecular crosslinking reactions and the lower temperatures in the heating zones.<sup>[37,40]</sup> For Tex-PAN 1, both wet- and dry-spun, EB-irradiated precursor fibers were stabilized. The tensile forces that occurred during the stabilization of EB-irradiated Tex-PAN 1 fibers were lower for dry-spun fibers compared to wet-spun fibers. This is likely due to the lower Young's modulus and the higher elongation of dry-spun compared to the wet-spun Tex-PAN 1 precursor fibers (Table 1). As a result, the dry-spun Tex-PAN 1 fibers were less prone to relaxation.<sup>[45]</sup>

In the stabilization trials with Tex-PAN 3, the tensile forces were generally higher than in the stabilization trials with Tex-PAN 1 and Tex-PAN 2, despite the lower stretching applied. Interestingly, the tensile forces of the irradiated fibers were higher only in heating zones 1 and 2, in heating zones 3 and 4 the unirradiated fibers built up higher tensile forces. **Table 4** summarizes the mechanical properties of the resulting OxPAN fibers. For Tex-PAN 1 and Tex-PAN 2, EB irradiation resulted in OxPAN fibers with higher tensile strength. For Tex-PAN 3 fibers, tensile strength did not increase within experimental error. In view of the standard deviations, EB had no effect on the Young's modulus of OxPAN fibers made of Tex-PAN 1 and Tex-PAN 2. In the case of Tex-PAN 3, the Young's modulus was reduced by 16% due to EB irradiation. Overall, EB irradiation led to higher elongation for all OxPAN fibers made of Tex-PAN.

## 2.3. Carbonization

Carbonization was carried out in a continuous carbonization plant consisting of a low temperature (LT) and a high

**Table 4.** Comparison of the properties of OxPAN fibers prepared from wet- or dry-spun Tex-PAN fibers, unirradiated and irradiated with a dose of 1000 kGy, respectively.

PAN	EB-Dose [kGy]	Tensile strength [MPa]	Young's modulus [GPa]	Elongation [%]	Diameter [ $\mu\text{m}$ ]	Density [ $\text{g mL}^{-1}$ ]
Tex-PAN 1	0	240 $\pm$ 40	6.9 $\pm$ 0.8	16.8 $\pm$ 3.4	10.7 $\pm$ 1.2	1.39
Tex-PAN 1 <sup>a)</sup>	1000	285 $\pm$ 30	6.8 $\pm$ 0.9	19.3 $\pm$ 4.0	11.4 $\pm$ 0.9	1.36
Tex-PAN 1 <sup>b)</sup>	1000	245 $\pm$ 20	6.5 $\pm$ 0.4	23.0 $\pm$ 5.1	10.2 $\pm$ 1.5	1.36
Tex-PAN 2	0	190 $\pm$ 10	6.3 $\pm$ 0.5	19.5 $\pm$ 2.7	10.7 $\pm$ 0.4	1.39
Tex-PAN 2	1000	210 $\pm$ 20	5.9 $\pm$ 0.2	25.7 $\pm$ 4.2	11.0 $\pm$ 1.0	1.36
Tex-PAN 3	0	290 $\pm$ 30	9.4 $\pm$ 0.7	13.3 $\pm$ 1.4	11.4 $\pm$ 0.8	1.36
Tex-PAN 3	1000	280 $\pm$ 20	7.9 $\pm$ 0.5	17.1 $\pm$ 2.5	11.5 $\pm$ 0.8	1.37

<sup>a)</sup> wet-spun; <sup>b)</sup> dry-spun.

**Table 5.** Mechanical properties of CFs resulting from continuous stabilization and carbonization of the irradiated and unirradiated Tex-PAN fibers.

Carbon fiber	EB dose [kGy]	Tensile strength [GPa]	Young's modulus [GPa]	Elongation [%]	Diameter [ $\mu\text{m}$ ]	Density [ $\text{g mL}^{-1}$ ]
Toray T300	Unknown	3.0 $\pm$ 0.4	197 $\pm$ 7	1.47 $\pm$ 0.15	7.3 $\pm$ 0.3	1.77
Tex-PAN 1	0	2.3 $\pm$ 0.4	196 $\pm$ 6	1.12 $\pm$ 0.20	6.8 $\pm$ 0.4	1.73
Tex-PAN 1 <sup>a)</sup>	1000	2.7 $\pm$ 0.6	206 $\pm$ 9	1.24 $\pm$ 0.25	7.0 $\pm$ 0.6	1.77
Tex-PAN 1 <sup>b)</sup>	1000	3.1 $\pm$ 0.6	193 $\pm$ 9	1.54 $\pm$ 0.29	6.5 $\pm$ 0.5	1.77
Tex-PAN 2	0	1.7 $\pm$ 0.4	145 $\pm$ 20	1.18 $\pm$ 0.30	7.4 $\pm$ 0.7	1.67
Tex-PAN 2	1000	2.6 $\pm$ 0.6	184 $\pm$ 6	1.38 $\pm$ 0.26	7.0 $\pm$ 0.5	1.71
Tex-PAN 3	0	2.7 $\pm$ 0.5	215 $\pm$ 11	1.07 $\pm$ 0.22	7.9 $\pm$ 0.6	1.77
Tex-PAN 3	1000	3.0 $\pm$ 0.7	212 $\pm$ 9	1.38 $\pm$ 0.30	7.3 $\pm$ 0.4	1.78

<sup>a)</sup> wet-spun; <sup>b)</sup> dry-spun.

temperature (HT) oven (Figure S2, Supporting Information). The final carbonization temperature was 1350 °C, the carbon content was between 95 and 96 wt% (see Table S3, Supporting Information). Since it can be advantageous to use a low stretching in the LT furnace, which can increase the Young's modulus of the resulting CFs,<sup>[46]</sup> stretching values between 0% and 5% were selected in the LT oven. Table 5 provides an overview of the mechanical properties of the synthesized CFs in comparison to those of a Toray T300 CF.

For wet-spun Tex-PAN 1 fibers, EB-irradiation led to an increase in the average tensile strength of the CFs from 2.25 to 2.65 GPa (+18%); for Tex-PAN 2 fibers the average tensile strength increased even from 1.7 to 2.6 GPa (+53%). In the case of Tex-PAN 3 fibers, EB irradiation resulted only in a moderate increase in the average tensile strength from 2.7 to 3.0 GPa (+11 %). The Young's modulus and elongation of CFs made of EB-treated Tex-PAN 1 and Tex-PAN 2 fibers also increased. CFs made from Tex-PAN 3 fibers, whether irradiated or unirradiated, had the same Young's modulus. For CFs made from Tex-PAN 1 and Tex-PAN 2 fibers, the density also increased by EB irradiation from 1.73 to 1.77  $\text{g mL}^{-1}$  and from 1.67 to 1.71  $\text{g mL}^{-1}$ , respectively. The densities of CFs made of irradiated and unirradiated Tex-PAN 3 fibers were virtually identical (1.77 and 1.78  $\text{g mL}^{-1}$ ). The highest tensile strength of 3.1  $\pm$  0.6 GPa was achieved with CFs made from irradiated dry-spun Tex-PAN 1 fibers, exceeding the tensile strength of a Toray T300 fiber. Its Young's modulus was also comparable within experimental error. CFs with 3 GPa tensile strength were also achieved with irradiated Tex-PAN 3 fibers, these CFs even exceeded the Young's modulus of the T300

fiber by 8%. To the best of our knowledge, this is another rare example of CFs obtained from Tex-PANs, which have mechanical properties comparable to the ones of a T300 fiber, the first one being CFs made by Jin et al. on the carbonization line of carbon nexus in Australia<sup>[47]</sup> However, Jin et al. used a precursor with an exceptionally high tensile strength of 1.3  $\pm$  0.2 GPa and Young's modulus of 26.9  $\pm$  1.1 GPa, which is more than twice the values of typical Tex-PAN fibers (see Table 1).

#### 2.4. Weibull Statistics of the CFs

In contrast to PAN fibers, CFs are brittle materials and crack near their elastic limit instead of deforming plastically.<sup>[48]</sup> According to the "weakest link theory" they always break at their weakest point.<sup>[49]</sup> In case of CFs, this is either a macroscopic (surface) defect like a taper or pore, or a microscopic defect in the turbostratic carbon structure.<sup>[50,51]</sup> The distribution of these defects in CFs is reflected by the Weibull statistics, which describe the distribution of tensile strength of materials whose fracture depends largely on statistically distributed defects in the material structure.<sup>[49,52]</sup>

Table 6 shows the Weibull strengths  $\sigma_0$  and the Weibull modulus  $m$  of the manufactured CFs and a Toray T300 CF, the corresponding Weibull plots are shown in Figures S5–S8, Supporting Information. Typical values for  $m$  for commercial CFs are between 4 and 10.<sup>[53,54]</sup> All measured CFs, i.e., the measured T300 fiber with  $m = 8.8$  and the CFs from the irradiated and unirradiated Tex-PANs with  $m = 4.5$ –6.4, were within the expected range. Thus,  $\sigma_0$  is 3.17 GPa for the T300 fiber while  $\sigma_0$  of the CFs made

**Table 6.** Summary of the determined Weibull strengths  $\sigma_0$  and the Weibull moduli  $m$  of the investigated CFs prepared from irradiated or unirradiated Tex-PAN, compared to a commercial Toray T300 CF.

Carbon fiber	EB-dose [kGy]	$\sigma_0$ [GPa]	$m$ [a. u.]	$R^2$ [a. u.]
Toray T300	Unknown	3.17	8.8	0.924
Tex-PAN 1	0	2.41	6.4	0.986
Tex-PAN 1	1000	2.86	5.6	0.962
Tex-PAN 1	1000	3.34	5.5	0.963
Tex-PAN 2	0	1.88	4.5	0.955
Tex-PAN 2	1000	2.82	4.8	0.940
Tex-PAN 3	0	2.91	6.0	0.955
Tex-PAN 3	1000	3.24	5.1	0.981

of dry-spun Tex-PAN 1 and Tex-PAN 3 reached 3.34 and 3.24 GPa, respectively, which is above the  $\sigma_0$ -value of a T300 fiber.

## 2.5. Morphology of the CFs

Figure 2 shows the morphologies of CFs spun from Tex-PAN fibers. Clearly, the fibril structure on the surface of the Tex-PAN fibers was retained in the resulting CFs. The cross section of CFs made of unirradiated Tex-PAN 2 fibers was smooth, in line with the by far lowest tensile strength (Table 5).

In contrast, the cross section and surface of CFs prepared from EB-irradiated, dry-spun Tex-PAN 1 fibers, which had the highest average tensile strength revealed a fibril structure (Figure 3). In addition, the typical “dumbbell shape” of the cross-section of dry-spun PAN fibers can be seen. For CFs, a circular fiber cross-section is usually aimed for, since this typically leads to the best mechanical properties of CFs.<sup>[55]</sup> However, an atypical fiber morphology as shown in Figures 2 and 3 can be beneficial in CF-composites, as it leads to a better CF-matrix adhesion achieved by a better physical interlocking between the CFs and the surrounding matrix compared to circular CFs.<sup>[56]</sup>

## 2.6. Wide-Angle X-Ray Scattering (WAXS) Analysis of CFs Derived from Tex-PAN

Recently, Zhang et al. investigated the microstructures of ox-PAN fibers derived from irradiated and unirradiated PAN, respectively, by WAXS; however, to the best of our knowledge, no such comparison has been made for the final CFs derived therefrom.<sup>[57]</sup> In CFs, the carbon mainly exists in form of a turbostratic modification similar to graphite, but with the graphene planes corrugated, curved, cross-linked, and with little long-range order.<sup>[56,58–60]</sup> Moreover, the graphite-like crystallites in this structure are only a few nm in size. The carbon crystallites are characterized by their crystallite dimensions  $L_{a\perp}$ ,  $L_{a\parallel}$ , and  $L_c$ , as well as the spacing between the graphene layers  $d_{002}$ . In CFs, the individual graphene planes have a  $d_{002}$ -value of usually about 0.34–0.36 nm. In a perfect graphite single crystal,  $d_{002}$  is 0.3354 nm.<sup>[58]</sup>  $L_{a\perp}$ ,  $L_{a\parallel}$ , and  $L_c$  can be determined by WAXS. The crystallite lengths of the graphene planes parallel to the CF axis ( $L_{a\parallel}$ ) and orthogonal to the CF axis ( $L_{a\perp}$ ) are usually not evaluated separately and are combined to  $L_a$  due to low scattering intensity and the imperfect orientation of CFs.

Table 7 summarizes the values for  $L_c$ ,  $L_a$ ,  $d_{002}$ ,  $N_c$  and the preferred orientation (P. O.) of the Tex-PAN-derived CFs together with those for a Toray T300 CF.  $L_c$ ,  $L_a$ , and  $N_c$  values differed only slightly for all these CFs. However, the differences in the  $d_{002}$  spacing deserve attention. The  $d_{002}$  values were generally smaller for the Tex-PAN fibers than for the Toray T300–CF. A lower  $d_{002}$ -value indicates a more defect-free, graphite-like CF structure. CFs prepared from EB-irradiated Tex-PAN 2 and Tex-PAN 1, had lower  $d_{002}$  values compared to CFs prepared from the corresponding unirradiated fibers. Surprisingly, the  $d_{002}$ -value of the CFs derived from dry-spun Tex-PAN 1 was significantly lower than the  $d_{002}$  values of the CFs derived from wet-spun Tex-PAN 1 indicating a very compact microstructure with less defects for dry-spun fibers. Vice versa, for Tex-PAN 3 the  $d_{002}$ -value was slightly higher for the CFs derived from EB-irradiated fibers.

The P.O.-values of the CFs derived from irradiated Tex-PANs were generally slightly higher, which corresponds to the higher Young’s modulus of these fibers (Table 5). CFs made of irradiated, wet-spun Tex-PAN 1 had a P.O. of 80%, virtually identical to the one of the Toray T300 fiber.

## 2.7. Influence of EB-Irradiation on the Stabilization Mechanism of (Tex-)PAN

In the literature, two main statements have been made concerning the influence of EB-irradiation on the stabilization of PAN and PAN-copolymers. First, the persistent radicals in PAN generated by EB-irradiation induce stabilization reactions at lower temperatures compared to unirradiated PAN.<sup>[27–30,32,35–38,40,61,62]</sup> Second, intermolecular crosslinking is more pronounced during the stabilization of EB-irradiated PAN compared to unirradiated PAN.<sup>[28,35–37,40,61]</sup>

The results of this work support both statements. Thus, DSC measurements (Figure 1) showed that  $T_{\text{onset-S}}$  is significantly reduced for both copolymers Tex-PAN 1 and Tex-PAN 2, as well as for the homopolymer Tex-PAN 3. After EB-irradiation, the thermal properties of Tex-PAN 1–3 were quite similar, indicating that for irradiated PAN the chemical composition of the precursor, i.e., the amount and type of comonomer(s) plays only a subordinate role in the stabilization mechanism. An EB-induced radical stabilization mechanism as suggested by Park et al.<sup>37</sup> is therefore plausible. This EB-induced radical stabilization mechanism starts at lower temperatures compared to the ionic stabilization mechanism induced by acidic comonomers or the radical mechanism induced by thermally generated radicals.<sup>[42,63,64]</sup> Consequently, the use of EB-irradiation allows for variations in the polymer design for CF-production in that both the nature and amount of comonomers can be tuned to the productivity of fiber spinning since they have only a minor influence on the thermal properties of the fibers and the stabilization mechanism. Conveniently, PANs tuned to the productivity of fiber spinning have been designed over the course of more than 70 years in textile industry, rendering Tex-PANs attractive CF-precursors.

Generally, EB-induced crosslinking can be followed by IR-spectroscopy. Accordingly, a characteristic absorption band at 1668  $\text{cm}^{-1}$  assigned to a  $-\text{HC}=\text{N}=\text{N}=\text{CH}-$  group was observed for stabilized, EB-irradiated PAN, which can be attributed to the intermolecular recombination of two imine-radicals formed by

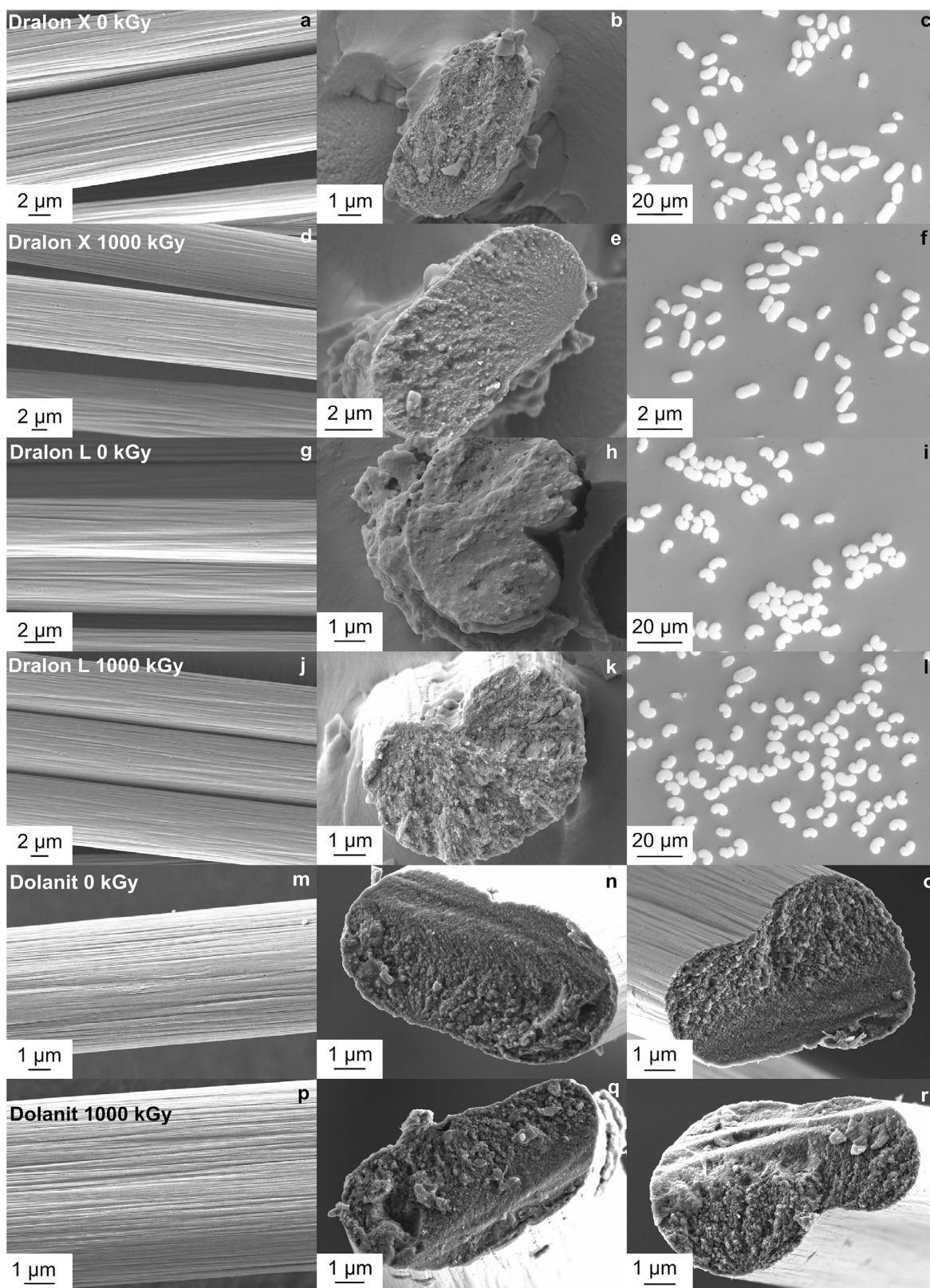


**Figure 2.** SEM images of the surface and cross section of the manufactured CFs derived from wet-spun Tex-PANs and some light microscope images of cross-sections of the final CFs embedded in epoxy resin (c, f, i, l). a–c) Tex-PAN 1 unirradiated. d–f) Tex-PAN 1 EB-irradiated with 1000 kGy. g–i) Tex-PAN 2 unirradiated. j–l) Tex-PAN 2 EB-irradiated with 1000 kGy. m–o) Tex-PAN 3 unirradiated. p–r) Tex-PAN 3 EB-irradiated at 1000 kGy.

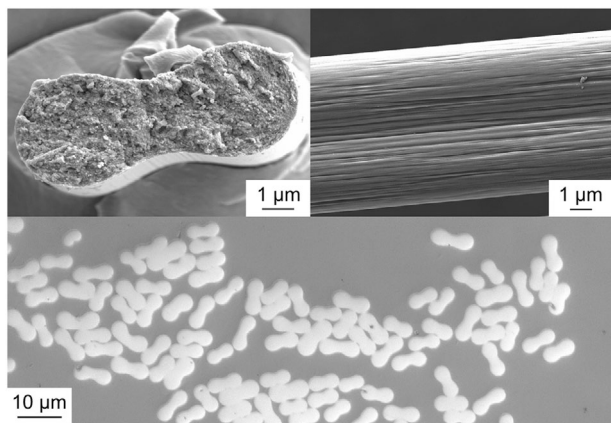


**Figure 3.** Top: SEM images of CFs made of 1000 kGy EB-irradiated, dry-spun Tex-PAN 1 fibers-Left: Cross section. Right: Surface. Bottom: Light microscope image of a microsection along the cross-section of those fibers embedded in an epoxy resin matrix.

**Table 7.** Structural properties of the CFs resulting from continuous stabilization and carbonization of EB-irradiated and unirradiated textile PAN fibers. Structural properties of a Toray T300 CF are shown for comparison, X-ray diffraction patterns shown in Figures S9–S15 (Supporting Information).

Carbon fiber	EB dose [kGy]	$L_c$ [nm]	$L_a$ [nm]	$d_{002}$ [nm]	$N_c$	P.O. [%]
Tex-PAN 1 (wet-spun)	0	1.36	2.91	0.353	3.8	78
Tex-PAN 1 (wet-spun)	1000	1.35	2.89	0.351	3.8	80
Tex-PAN 1 (dry-spun)	1000	1.29	2.76	0.347	3.7	79
Tex-PAN 2	0	1.24	2.67	0.356	3.5	75
Tex-PAN 2	1000	1.35	2.89	0.353	3.8	77
Tex-PAN 3	0	1.19	2.55	0.346	3.4	79
Tex-PAN 3	1000	1.24	2.68	0.347	3.6	80
Toray T300		1.29	2.63	0.359	3.6	81

EB-irradiation.<sup>[28,40,61]</sup> The results of the present work support this crosslinking hypothesis. The significantly higher tensile forces during stabilization, especially at the beginning of the stabilization in the first two heating zones, suggest that the intermolecular crosslinking of polymer chains is more pronounced for irradiated PANs compared to their unirradiated analogs (Table 3). Despite identical stretching ratios during stabilization and carbonization, an increase in P.O. of the CFs was observed by WAXS for irradiated PAN compared to CFs derived from unirradiated PAN and can also be explained by crosslinking. Thus, crosslinking “freezes” the orientation of the polymer chains in the precursor fiber thereby reducing chain mobility. As a result, the polymer chain orientation in the precursor fiber is better preserved in the resulting CFs.

### 3. Conclusion

Tex-PANs with low comonomer content are suitable precursors for CF-production if they are EB-irradiated prior to stabilization. CFs prepared from Tex-PAN 1 (copolymer) and Tex-PAN 3 (homopolymer) have mechanical properties similar or better than Toray T300 fibers. The irradiation and carbonization of dry-spun

Tex-PAN 1 lead to CFs with better mechanical properties and a more compact microstructure compared to CFs derived from wet-spun Tex-PAN 1. It was shown that EB-irradiation of Tex-PANs leads to a superior microstructure of the CFs compared to those derived from unirradiated Tex-PANs. By EB irradiation, significantly lower  $d_{002}$  values and higher P. O. values can be achieved. The investigated Tex-PANs are suitable for CF production, provided EB irradiation is applied, and the estimated costs added by EB-irradiation are in the range of 0.3–0.4 \$ kg<sup>-1</sup>, which is by far outweighed by the cost benefit of Tex-PAN precursor fibers over typical PAN-based precursor fibers.

### 4. Experimental Section

**Textile-Grade PAN Precursors:** The Tex-PAN 3K multifilaments used in this work were kindly provided by Dralon GmbH. Three different Tex-PANs were investigated: Tex-PAN 1 (96.0 mol% acrylonitrile, 0.2 mol% sodium methallyl sulfonate, 3.8 mol% methyl acrylate), Tex-PAN 2 (95.9 mol% acrylonitrile, 4.1 mol% vinyl acetate) and Tex-PAN 3 (100 mol% acrylonitrile). The Tex-PAN 1 fibers used in this work were wet- and dry-spun, Tex-PAN 2 and Tex-PAN 3 fibers were wet-spun.

**Characterization:** For mechanical testing of the fibers, 20 (precursor, stabilized fibers) or 30 (CFs) single filament measurements were conducted on a Favimat, Texttechno. The clamping length was 25 mm, the test speed was 20 mm min<sup>-1</sup> (precursor), 10 mm min<sup>-1</sup> (stabilized fibers), or 1 mm min<sup>-1</sup> (CFs). SEM micrographs were taken on a Zeiss Auriga scanning electron microscope using a Quorum Technologies sputter with a Pt/Pd Target. Samples were sputtered with 5 nm of Pt/Pd. Micrographs were taken at acceleration voltages of 3 kV and working distances between 6 and 8 mm in the secondary electron mode (Everhardt-Thornley detector). X-ray scattering was measured on a D/MAX Rapid II manufactured by Rigaku, using 40 kV and 30 mA Cu-K<sub>α</sub>-irradiation ( $\lambda = 0.15406$  nm). A shine monochromator and an image plate detector were used. The scanning rate was 0.2° min<sup>-1</sup>; the scanning step was 0.1°. All fibers were aligned in a fiber sample holder. The crystallinity was calculated on the basis of the following formula:

$$I_c = \frac{\sum I_c}{\sum (I_c + I_a)} \quad (1)$$

in which  $I_c$  is the intensity of the crystalline reflections and  $I_a$  is the intensity of the amorphous reflections. For integration of the peak areas, the method developed by Gupta and Singhal was used.<sup>[65]</sup> The preferred orientation (P. O.) of the crystallites of PAN was calculated according to:

$$P.O. = \frac{180^\circ - B}{180^\circ} \quad (2)$$

where  $B$  is the full width at half maximum (FWHM) of the (100) reflection of the hexagonal lattice of PAN.<sup>[65]</sup> The crystallite length  $L_a$  and the crystallite thickness  $L_c$  were determined according to the Scherrer equation

$$L = \frac{K \cdot \lambda}{B \cdot \cos \theta} \quad (3)$$

In which  $K$  represents the crystallite shape-dependent shear factor. For  $L_a$ ,  $K$  is 0.9, for  $L_c$ ,  $K$  is 1.83.<sup>[66]</sup> The average number of graphene layers  $N_c$  in a crystallite was calculated from the ratio  $L_c/d_{002}$ . Differential scanning calorimetry (DSC) measurements were carried out under air on a TA Instruments Q2000 differential scanning calorimeter with a heating rate of 10 K min<sup>-1</sup>. Size exclusion chromatography (SEC) measurements were performed on a 1260 Infinity device from Agilent Technologies equipped with a Multi-Detector-Suite viscosimetry and a refractive index detector. A 50 mm precolumn and a 300 mixed B column (Agilent Technologies) were used as stationary phase, DMAc containing 5 g L<sup>-1</sup>

LiBr was used as mobile phase. The column temperature was set to 50 °C, the flow rate was 0.75 L min<sup>-1</sup>, the sample concentration was 2 mg mL<sup>-1</sup>. Chromatograms were interpreted using conventional calibration against poly(methyl methacrylate) polymer standards. Density measurements were carried out by placing a fiber sample in various mixtures of halogenated solvents with a defined density in steps of 0.01 g mL<sup>-1</sup>. The density of the mixture in which fibers neither sunk nor surfaced but floated for > 10 min was assigned to the fibers. Elemental analyses were measured on a Perkin Elmer 240 device.

**Electron-Beam (EB) Irradiation:** EB Irradiation was carried out on an EC-LAB 400, Electron Crosslinking AB, configured for continuous irradiation. The EB current was 3.5 mA, the acceleration voltage was 200 keV, the winding speed was 6.7 m min<sup>-1</sup> (Photograph of PAN-fibers prior to and after EB irradiation are shown in Figure S3, Supporting Information).

**Stabilization:** Stabilization was performed in air on a continuous stabilization line by Dienes Apparatebau GmbH consisting of four heating ovens. In all four ovens, stretching ratios were applied and the apparent tensile forces were monitored. The winding speed was 0.9 m min<sup>-1</sup>. The stabilization furnace used in this work is shown in Figure S1 (Supporting Information). The total dwell length of the filament in the ovens was 66.0 m. The dwell time of the multifilament in the ovens at the utilized stretching ratios and winding speed was 75 min for Tex-PAN 1 and Tex-PAN 2, and 72 min for Tex-Pan 3, respectively.

**Carbonization:** Carbonization was performed under nitrogen on a continuous carbonization line from Gero Hochtemperaturöfen GmbH, consisting of a low temperature (LT) and a high temperature (HT) oven. The LT oven had six consecutive heating zones operating at 300, 390, 480, 570, 660, and 750 °C, respectively (Table S1, Supporting Information). The HT oven had three consecutive heating zones at 1000, 1175, and 1350 °C (Table S2, Supporting Information). In both ovens, different stretching ratios were applied. For all carbonization trials, the stretching ratio in the HT oven was set to -3.5%. The winding speed was 0.75 m min<sup>-1</sup>. Figure S2 (Supporting Information) shows a schematic representation of the carbonization line, which consisted of a low-temperature (LT) and a high-temperature (HT) furnace.

## Supporting Information

Supporting Information is available from the Wiley Online Library or from the author.

## Acknowledgements

The authors thank Ulrich Hageroth and Sabine Henzler for SEM measurements and Dr. Antje Ota and Dr. Tanja Schneck for WAXS measurements. Financial support provided by Dralon GmbH is gratefully acknowledged.

Open Access funding enabled and organized by Projekt DEAL.

## Conflict of Interest

The authors declare no conflict of interest.

## Data Availability Statement

Research data are not shared.

## Keywords

carbon fibers, electron beam, PAN, poly(acrylonitrile), textiles

Received: July 1, 2021

Revised: August 25, 2021

Published online: September 16, 2021

- [1] P. Bajaj, A. K. Roopanwal, *J. Macromol. Sci., Polym. Rev.* **1997**, *37*, 97.
- [2] E. Frank, F. Hermanutz, M. R. Buchmeiser, *Macromol. Mater. Eng.* **2012**, *297*, 493.
- [3] E. Frank, L. M. Steudle, D. Ingildeev, J. M. Spörl, M. R. Buchmeiser, *Angew. Chem., Int. Ed.* **2014**, *126*, 5364.
- [4] B. A. Newcomb, *Composites, Part A* **2016**, *91*, 262.
- [5] M. Sauter, M. Kühnel, *The Global CF and CCMarket 2018—Market developments, trends, outlook and challenges (CCeV)*, Carbon Composites eV, **2018**, [https://composites-united.com/media/3988/eng\\_cccv\\_market-report\\_2019\\_short-version.pdf](https://composites-united.com/media/3988/eng_cccv_market-report_2019_short-version.pdf).
- [6] J. Donnet, R. Bansal, *Carbon Fibers*, CRC Press, Boca Raton, FL **1998**.
- [7] C. Soutis, *Mater. Sci. Eng., A* **2005**, *412*, 171.
- [8] S. Nunna, P. Blanchard, D. Buckmaster, S. Davis, M. Naebe, *Heliyon* **2019**, *5*, e02698.
- [9] M. G. W. Abdallah, C. David; C. Joseph, *Automotive Lightweight Materials FY 2004 Progress Report*, Department of Energy, Washington DC, USA **2004**.
- [10] A. S. Gill, D. Visotsky, L. Mears, J. Summers, *J. Manuf. Sci. Eng.* **2017**, *139*, 041011.
- [11] H. Khayyam, R. N. Jazar, S. Nunna, G. Golkarnareni, K. Badii, S. M. Fakhrohoseini, S. Kumar, M. Naebe, *Prog. Mater. Sci.* **2020**, *107*, 100575.
- [12] C. Wang, R. A. Venditti, *ACS Sustainable Chem. Eng.* **2015**, *3*, 1839.
- [13] T. Wells, M. Kosa, A. J. Ragauskas, *Ultrason. Sonochem.* **2013**, *20*, 1463.
- [14] L. M. Steudle, E. Frank, A. Ota, U. Hageroth, S. Henzler, W. Schuler, R. Neupert, M. R. Buchmeiser, *Macromol. Mater. Eng.* **2017**, *302*, 1600441.
- [15] M. Culebras, A. Beaucamp, Y. Wang, M. M. Claus, E. Frank, M. N. Collins, *ACS Sustainable Chem. Eng.* **2018**, *6*, 8816.
- [16] J. M. Spörl, A. Ota, S. Son, K. Massonne, F. Hermanutz, M. R. Buchmeiser, *Mater. Today Commun.* **2016**, *7*, 1.
- [17] J. M. Spörl, R. Beyer, F. Abels, T. Cwik, A. Müller, F. Hermanutz, M. R. Buchmeiser, *Macromol. Mater. Eng.* **2017**, *302*, 1700195.
- [18] B. E. Barton, M. J. Behr, J. T. Patton, E. J. Hukkanen, B. G. Landes, W. Wang, N. Horstman, J. E. Rix, D. Keane, S. Weigand, M. Spalding, C. Derstine, *Small* **2017**, *13*, 1701926.
- [19] J.-S. Tsai, C.-H. Lin, *J. Appl. Polym. Sci.* **1991**, *43*, 679.
- [20] J.-S. Tsai, C.-H. Lin, *J. Appl. Polym. Sci.* **1991**, *42*, 3045.
- [21] E. A. Morris, M. C. Weisenberger, M. G. Abdallah, F. Vautard, H. Grappe, S. Ozcan, F. L. Paulauskas, C. Eberle, D. Jackson, S. J. Mecham, A. K. Naskar, *Carbon* **2016**, *101*, 245.
- [22] A. Jacob, *Reinf. Plast.* **2014**, *58*, 18.
- [23] B. S. Gupta, M. Afshari, in *Handbook of Properties of Textile and Technical Fibres*, 2nd ed. (Ed: A. R. Bunsell), Woodhead Publishing, Sawston, UK **2018**, p. 545.
- [24] F. Paulauskas, C. Warren, C. Eberle, A. Naskar, S. Ozcan, A. Fagundes, R. Dias, P. de Magalhães, in *17th Int. Committee on Composite Materials ICCM*, International Committee on Composite Materials, Edinburgh, UK **2009**.
- [25] S. Park, H.-S. Kil, D. Choi, S.-K. Song, S. Lee, *J. Ind. Eng. Chem.* **2019**, *69*, 449.
- [26] S.-Y. Kim, S. Y. Kim, S. Lee, S. Jo, Y.-H. Im, H.-S. Lee, *Polymer* **2015**, *56*, 590.
- [27] J. Dietrich, P. Hirt, H. Herlinger, *Eur. Polym. J.* **1996**, *32*, 617.
- [28] P. Miao, D. Wu, K. e Zeng, G. Xu, C. E. Zhao, G. Yang, *Polym. Degrad. Stab.* **2010**, *95*, 1665.
- [29] H. Yu, H. Yuan, Y. Wang, Z. Wei, G. Xia, *J. Wuhan Univ. Technol., Mater. Sci. Ed.* **2013**, *28*, 574.
- [30] H. K. Shin, M. Park, P. H. Kang, H.-S. Choi, S.-J. Park, *J. Ind. Eng. Chem.* **2014**, *20*, 3789.



- [31] L. Zhou, Y. Lu, W. Zhao, C. Yang, J. Jiang, *Polym. Degrad. Stab.* **2016**, 128, 149.
- [32] J. Yang, Y. Liu, J. Liu, Z. Shen, J. Liang, X. Wang, *Materials* **2018**, 11, 1270.
- [33] A. Y. Jo, S. H. Yoo, Y.-S. Chung, S. Lee, *Carbon* **2018**, 11, 1270.
- [34] U. Gohs, R. Böhm, H. Brüning, D. Fischer, L. Häussler, M. Kirsten, M. Malanin, M.-T. Müller, C. Cherif, D. S. J. Wolz, H. Jäger, *Radiat. Phys. Chem.* **2019**, 156, 22.
- [35] W. Zhang, M. Wang, W. Liu, C. Yang, G. Wu, *Polym. Degrad. Stab.* **2019**, 167, 201.
- [36] S. H. Yoo, S. Park, Y. Park, D. Lee, H.-I. Joh, I. Shin, S. Lee, *Carbon* **2017**, 118, 106.
- [37] S. Park, S. H. Yoo, H. R. Kang, S. M. Jo, H.-I. Joh, S. Lee, *Sci. Rep.* **2016**, 6, 27330.
- [38] W. Zhang, M. Wang, W. Zhang, W. Liu, C. Yang, R. Shen, G. Wu, *Polym. Degrad. Stab.* **2018**, 158, 72.
- [39] A. Sedghi, R. E. Farsani, A. Shokuhfar, *J. Mater. Process. Technol.* **2008**, 198, 60.
- [40] Y. Liu, X. Huang, J. Liu, J. Liang, X. Wang, *J. Mater. Sci.* **2020**, 55, 4962.
- [41] E. A. Morris, M. C. Weisenberger, S. B. Bradley, M. G. Abdallah, S. J. Mecham, P. Pisipati, J. E. McGrath, *Polymer* **2014**, 55, 6471.
- [42] Q. Ouyang, L. u Cheng, H. Wang, K. Li, *Polym. Degrad. Stab.* **2008**, 93, 1415.
- [43] S. Nunna, M. Naebe, N. Hameed, B. L. Fox, C. Creighton, *Polym. Degrad. Stab.* **2017**, 136, 20.
- [44] J. Mittal, H. Konno, M. Inagaki, O. P. Bahl, *Carbon* **1998**, 36, 1327.
- [45] T. Shen, C. Li, B. Haley, S. Desai, A. Strachan, *Polymer* **2018**, 155, 13.
- [46] N. V. Salim, S. Blight, C. Creighton, S. Nunna, S. Atkiss, J. M. Razal, J. M. Razal, *Ind. Eng. Chem. Res.* **2018**, 57, 4268.
- [47] X. Jin, C. Feng, C. Creighton, N. Hameed, J. Parameswaranpillai, N. V. Salim, *Polym. Degrad. Stab.* **2021**, 186, 109536.
- [48] S. van der Zwaag, *J. Test. Eval.* **1989**, 17, 292.
- [49] W. Weibull, *R. Swed. Inst. Eng. Res.* **1939**, 151, 1.
- [50] F. W. Zok, *J. Am. Ceram. Soc.* **2017**, 100, 1265.
- [51] T. Tagawa, T. Miyata, *Mater. Sci. Eng., A* **1997**, 238, 336.
- [52] W. Weibull, *J. Appl. Mech.* **1951**, 18, 293.
- [53] J. Hitchon, D. Phillips, *Fibre Sci. Technol.* **1979**, 12, 217.
- [54] K. Naito, Y. Tanaka, J.-M. Yang, Y. Kagawa, *Carbon* **2008**, 46, 189.
- [55] S.-J. Park, M.-K. Seo, H.-B. Shim, K.-Y. Rhee, *Mater. Sci. Eng., A* **2004**, 366, 348.
- [56] W. Li, D. Long, J. Miyawaki, W. Qiao, L. Ling, I. Mochida, S.-H. o Yoon, *J. Mater. Sci.* **2012**, 47, 919.
- [57] W. Zhang, M. Wang, L. i Cheng, G. Wu, *Polym. Degrad. Stab.* **2020**, 179, 109264.
- [58] E. A. Belenkov, *Inorg. Mater.* **2001**, 37, 928.
- [59] D. J. Johnson, *J. Phys. D: Appl. Phys.* **1987**, 20, 286.
- [60] S. C. Bennett, D. J. Johnson, *Carbon* **1979**, 17, 25.
- [61] J. H. Lee, J.-U. Jin, S. Park, D. Choi, N.-H. You, Y. Chung, B.-C. Ku, H. Yeo, *J. Ind. Eng. Chem.* **2018**, 71, 112.
- [62] H. Xiao, P. K. Miao, *Mater. Sci. Forum* **2020**, 996, 35.
- [63] J. Kim, Y. C. Kim, W. Ahn, C. Y. Kim, *Polym. Eng. Sci.* **1993**, 33, 1452.
- [64] M. Yu, C. Wang, Y. Bai, Y. Wang, B. o Zhu, *J. Appl. Polym. Sci.* **2006**, 102, 5500.
- [65] A. K. Gupta, R. P. Singhal, *J. Polym. Sci., Polym. Phys. Ed.* **1983**, 21, 2243.
- [66] B. E. Warren, P. Bodenstern, *Acta Crystallogr.* **1966**, 20, 602.